Title

Quantitative studies of wildfire smoke injection heights with the Terra Multi-angle Imaging SpectroRadiometer

ISBN

978-0-8194-7309-7

Authors

Diner, David J
Nelson, David L
Chen, Yang
et al.

Publication Date

2008-08-28

DOI

10.1117/12.795215

Quantitative studies of wildfire smoke injection heights with the Terra Multi-angle Imaging SpectroRadiometer

David J. Diner*[a], David L. Nelson[a], Yang Chen[a], Ralph A. Kahn[b], Jennifer Logan[c], Fok-Yan Leung[d], and Maria Val Martin[c]
[a]Jet Propulsion Laboratory, California Institute of Technology
[b]NASA Goddard Space Flight Center
[c]Harvard University
[d]Washington State University

ABSTRACT

The Multi-angle Imaging SpectroRadiometer (MISR) is in its ninth year of operation aboard NASA's Terra satellite. MISR acquires imagery at nine view angles between 70.5º forward and backward of nadir. Stereoscopic image matching of red band data at 275-m horizontal spatial resolution provides measurements of aerosol plume heights in the vicinity and downwind of wildfires. We are supplementing MISR's standard stereo product with more detailed, higher vertical spatial resolution stereo retrievals over individual smoke plumes, using the MISR INteractive eXplorer (MINX) analysis tool. To limit the amount of data that must be processed, MODIS (Moderate resolution Imaging Spectroradiometer) thermal anomaly data are used to identify fire locations. Data over North America are being analyzed to generate a climatology of smoke injection heights and to derive a general parameterization for the injection heights that can be used within non-plume-resolving chemical transport models. In 2002, we find that up to about 30% of fire plumes over North America reached the free troposphere. Sufficiently buoyant plumes tend to become trapped near stratified stable layers within the atmospheric vertical profile, supporting a result first obtained on a more limited set of MISR data [1]. Data from other years are being processed to further establish the robustness of these conclusions.

Keywords: wildfires, smoke, plumes, stereo imaging, MISR

1. INTRODUCTION

Data from surface stations and Earth-orbiting spacecraft provide compelling evidence that regional air quality is influenced by events transpiring a great distance away. In July 2002, for example, smoke from large wildfires in Quebec was transported rapidly down the eastern coast of the U.S., reducing visibility and dramatically affecting air quality [2], [3]. In May 1998, visibility in the U.S. was affected by smoke from catastrophic fires in Mexico and Central America, with the smoke pall extending eastward from New Mexico to southern Florida, and as far north as Wisconsin [4]-[6]. The frequency of wildfires has increased over the past few decades [7], and they may be even more common in a future, warmer climate [8]. Predicting the effects of climate change on air quality requires the ability to accurately model smoke injection and long-range transport.

Models and observations (e.g., [9], [10]) show that aerosol residence times in the atmosphere and downwind effects on surface air quality depend on the heights at which emissions are injected. In a study of 1998 boreal fires, Leung et al. [11] concluded on the basis of chemical transport modeling using GEOS-CHEM that at least half of the CO emission needed to be injected above the boundary layer (typically to altitudes of 3-5 km) in order to account for downwind column CO abundances, which were elevated by 30% above normal. It is well known that crown fires generate sufficient energy to loft smoke plumes above the boundary layer [12], [13]. Case studies have shown that smoke from large fires can be injected to stratospheric altitudes by supercell convection [14], [15]. Using aerosols as a tracer, satellite observations of plume injection heights from wildfires help us determine the frequency distribution of smoke injection to various altitudes. One of our primary goals is to generate an observationally-constrained parameterization for the injection heights of biomass burning emissions from forest fires that can be used in global atmospheric models.

*David.J.Diner@jpl.nasa.gov; phone 1 818 354-6319; fax 1 818 393-4619

Remote Sensing of Fire: Science and Application, edited by Wei Min Hao,
Proc. of SPIE Vol. 7089, 708908, (2008) · 0277-786X/08/$18 · doi: 10.1117/12.795215

2. OBSERVATIONAL METHODOLOGY

Satellite lidar, e.g., the CALIOP (Cloud-Aerosol Lidar with Orthogonal Polarization) lidar [16] flying in polar orbit aboard the CALIPSO (Cloud-Aerosol Lidar and Infrared Pathfinder Satellite Observations) satellite, is one method of measuring smoke altitude at a large number of locations. Although lidars provide unequaled details on aerosol vertical profiles, they have limited coverage, observing only along narrow swaths. An alternative method is through passive stereoscopic imagery, which provides the heights of the tops of aerosol layers or plumes provided that sufficient spatial contrast exists for multiangle image pattern matching to work. Pattern matching of images acquired at different view angles provides a measure of disparity, i.e., the horizontal displacement of image features due to their elevation above the surface (also known as parallax). The satellite orbit parameters and camera geometric model are then used to translate the disparities into heights. As a purely geometric technique, stereo height retrievals are independent of assumptions about the atmospheric temperature profile or composition of the scatterers, and can be performed over a wide swath. With over eight years of data from the Multi-angle Imaging SpectroRadiometer (MISR) instrument on NASA's Earth Observing System (EOS) Terra satellite, long-term monitoring of cloud and aerosol heights using automated global stereo retrievals has now been made possible.

MISR [17] acquires multiangle radiance imagery from a set of nine pushbroom cameras, with the forward and backward viewing cameras paired in a symmetrical arrangement at a fixed set of view angles. Relative to the Earth's surface, the along-track angles are nominally 0º (nadir) and 26.1º, 45.6º, 60.0º, and 70.5º forward and backward of nadir. During a 7-minute interval, each point within the instrument swath is viewed in succession by the nine cameras as the spacecraft flies overhead. Camera focal lengths range from 59 mm to 124 mm, keeping cross-track pixel size and sample spacing to 250 m for the nadir camera and 275 m for the off-nadir cameras. Sample spacing in the along-track direction is 275 m in all cameras as a consequence of the 40.8-msec line repeat time of the CCD (charge-coupled device) readouts. Each MISR camera contains four CCD line arrays with 21 μm detector pitch, and a focal plane filter assembly is mounted above the CCDs to define the four bandpasses, centered at 446, 558, 672, and 866 nm. Coregistration of the data in both band and angle is accomplished in ground data processing [18]. MISR radiances are geolocated on a Space Oblique Mercator (SOM) grid. Geolocation uncertainty is estimated to be ±50 m, and coregistration errors are < 275 m.

MISR standard stereo products provide contiguous global coverage of heights at or near the tops of clouds, aerosol plumes, and optically thick aerosol layers [19], [20]. Red-band (672 nm) data from the nadir and 26.1º cameras are used operationally for this purpose. In the standard MISR stereo product, the quantized precision of the retrieved height field is ±560 m. Altitudes for clouds as wells as smoke and dust plumes are reported on a 1.1-km resolution horizontal grid. Validations using ground-based 35/94 GHz radar and lidar retrievals suggest uncertainties of < 1 km [21]-[23]. Since the technique is purely geometric, comparable accuracy is expected for aerosol layers.

One complication for stereo height retrieval is that the component of cloud and aerosol plume advection in the along-track direction results in a spatial displacement of the features due to the actual atmospheric motion, in addition to the height-related parallax. Stereo imaging using at least three angles makes possible a novel technique for separating these two effects and determining height-resolved atmospheric motion vectors [24], [25]. The technique is used operationally for MISR product generation. In the MISR standard stereo product, "zero-wind heights" are computed assuming that feature displacements between different view angles are due entirely to parallax. "Best-wind heights" make use of wind retrievals from the nadir-45.6º-70.5º camera triplet and the nadir-45.6º-70.5º backward camera triplet, with the requirement that the results must be similar to within a specified tolerance. Winds are retrieved at 70.4-km resolution, making use of many matched features within these mesoscale domains. Both zero-wind and best-wind heights are reported on 1.1-km centers. Because of the quality control applied to the wind retrievals, coverage is typically much better for the zero-wind product. The MISR standard stereo product, and the multiangle radiance imagery from which the heights and winds are derived, are available from the NASA Langley Atmospheric Sciences Data Center.

3. DATA PROCESSING

3.1 Large-scale processing

The global MISR stereo product contains retrievals of the heights of innumerable aerosol plumes, not only from wildfires but also volcanic eruptions and dust clouds. An example stereo plume height retrieval from MISR's publicly available standard product is shown in Fig. 1. The data show smoke from wildfires in southern California on 26 October 2003. Plumes are apparent from fires burning near the California-Mexico border, San Diego, Camp Pendleton, the foothills of the San Bernardino Mountains, and in and around Simi Valley. The left panel is a nadir camera image and the

panel to the right of the image was generated from the standard stereo product. Typical smoke altitudes are near 3 km. The red patches are high cirrus, which are visually similar to the smoke in the nadir image but are clearly separable by their retrieved altitude. The right-hand panel of Fig. 1 is the atmospheric stability profile, calculated as the vertical gradient of potential temperature from the National Centers for Environmental Prediction (NCEP) Global Data Analysis System. Case studies of MISR stereo heights near active fires have been used to investigate the relationship between atmospheric stability and plume altitudes. Kahn et al. [1] suggested that plumes tend to concentrate in layers of enhanced atmospheric stability based on such analysis. Indeed, the region of enhanced stability in the example shown in Fig. 1 encompasses the heights at which the smoke is concentrated.

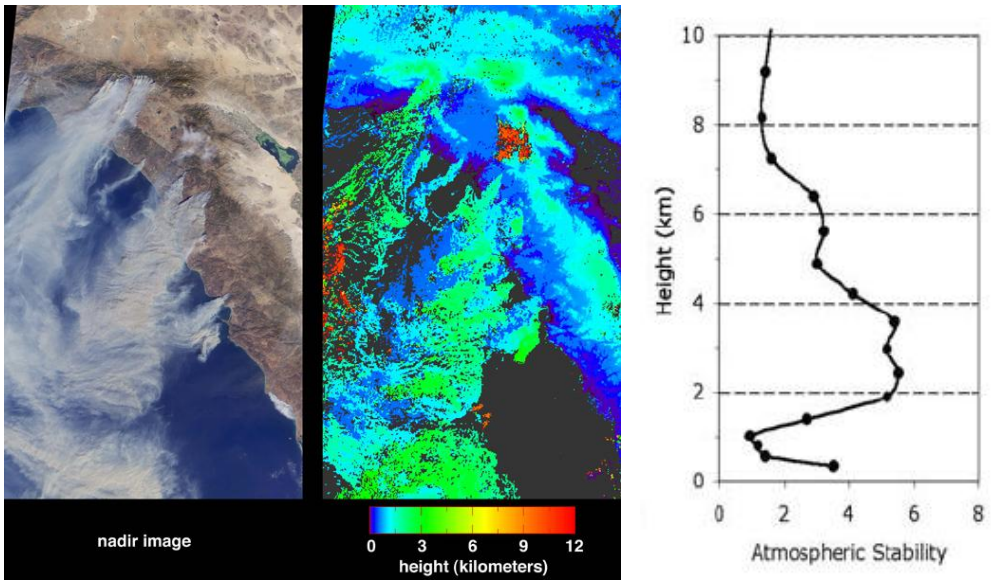

Figure 1. Left: MISR nadir image of wildfire smoke plumes in southern California, Terra orbit 20510, path 40. Middle: Visualization of standard stereo product height retrievals. Right: Atmospheric stability profile derived from NCEP data (adapted from [1]).

Using MISR data from 19 January 2003, Fig. 2 shows stereo retrievals of smoke far from the source. The smoke originated from extensive bushfires in the Australian Capital Territory. The area shown is ~1600 km east of Canberra. This figure illustrates that with near-nadir stereo imagery of diffuse smoke, the aerosol plumes may not always contain adequate contrast for pattern matching to work. This can often be resolved by running the height retrievals on imagery from the oblique-angle (e.g., 45.6º, 60.0º, or 70.5º) cameras. The second and third panels of Fig. 2 compare the results of near-nadir with oblique stereo. At the oblique angles, the enhanced optical path is sufficient to enable stereo height determinations on at least some portion of the plumes that are otherwise too thin for the nadir and near-nadir views to obtain a match. In Fig. 2, the thin, "low smoke" is missed by the near-nadir cameras but a sliver of green (corresponding to heights near 5 km) in the oblique-camera retrieval shows that the edge of this plume has been detected. Note that despite the similar visual appearance of the thin smoke and cirrus, they are again readily distinguished by their heights, as in Fig. 1. Both stereo retrievals detect the thicker "high smoke" but coverage is better when the oblique cameras are used. Since the search windows to find pattern matches are much larger when the oblique cameras are used, the retrievals are more computationally expensive. As a result, oblique-camera stereo results are not generated routinely and have been run only on a case-by-case basis at the MISR Science Computing Facility at JPL. This approach was used in an analysis of incursion of smoke from the May 2001 Chisholm Fire (Alberta, Canada) into the lower stratosphere [15] and to study plume dispersal following collapse of the World Trade Center on 11 September 2001 [26].

Figure 3 is a normalized frequency histogram of the oblique-camera stereo heights retrieved from the top one-third of the scene shown in Fig. 2. We associate the two maxima in the histogram near 4.5 km and 6 km with the low smoke, and the large peak at 8 km with the high smoke. These heights have not been adjusted for the effects of any along-track component of atmospheric motion (cross-track motion does not affect the parallax measurement). Since the height retrievals with the wind correction are noisier and have poorer coverage than the uncorrected retrievals, a regression analysis was used to determine the magnitude of the height difference associated with correction for wind. We find that the wind-corrected heights on average are within 500 m of the uncorrected heights.

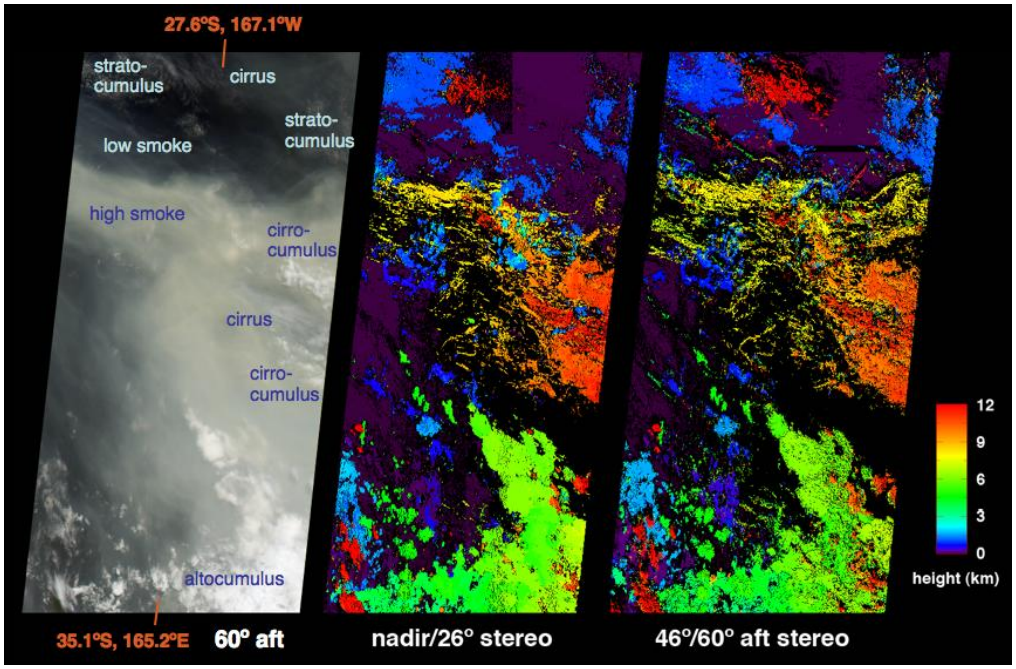

Figure 2. Left: Image from MISR's 60º backward-viewing camera acquired on 19 January 2003 at around 2306Z. The swath is about 400 km wide. The scene is multi-layered, with clouds and smoke at a variety of altitudes. Middle: Stereo height retrievals from MISR standard processing, which makes use of the nadir and near-nadir cameras. Right: Stereo height retrievals using specialized processing, employing the same algorithms as in standard processing but with imagery from the 45.6º and 60º aft-viewing cameras. Data are from Terra orbit 16435, path 80, MISR blocks 113-118.

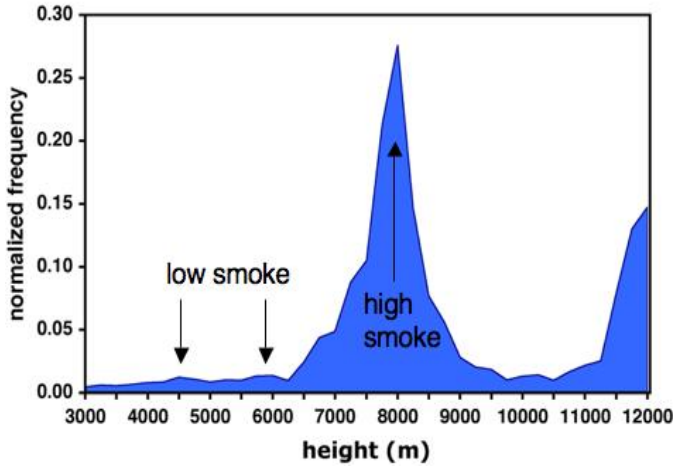

Figure 3. Normalized frequency histogram of the oblique-camera stereo heights retrieved from the top portion of the scene in Fig. 2. The heights have not been corrected for wind effects; in this scene the corrections are typically < 500 m.

3.2 Processing using the MISR INteractive eXplorer (MINX)

In the interest of developing a parameterization for smoke injection altitudes in transport models and to isolate those surface or atmospheric parameters that are the most significant predictors of injection height, we developed a system for mining the MISR data to generate a statistically meaningful data set. Given that the standard processing retrieves wind vectors on 70.4-km domains, which is often too coarse for making wind corrections on localized plumes, our goal was to enable higher-resolution retrievals in the vicinity of wildfire plumes. Since plume orientation is a good indicator of wind direction, one degree of freedom can be dropped from the retrievals, and stereo pairs rather than triplets are adequate to determine plume height and wind speed [27].

An initial processing system for mining MISR data for plume height determination made use of thermal anomaly data from the Terra Moderate resolution Imaging Spectroradiometer (MODIS) to locate active fires, which resulted in orders of magnitude reduction in the amount of data that needed to be analyzed [28]. Our initial objective was to retrieve plume parameters (e.g., height and orientation) without any human interaction, but we found that a purely automated system was too limiting in the number of plumes for which reliable results could be obtained. As a consequence, a semi-automated system was put in place, and the MISR INteractive eXplorer (MINX) analysis software package [27] was developed to improve upon the earlier climatology. The use of MODIS thermal anomaly data to locate active fires is retained, and a number of algorithmic enhancements that cannot (due to processing speed limitations) be implemented in generation of the MISR global stereo product have been implemented, as described in Nelson et al. [27]. The results of this MISR Plume Height Climatology Project are publicly available on the World Wide Web at http://www-misr2.jpl.nasa.gov/EPA-Plumes/. Currently, data over Alaska from 2004, and data over North America for 2002 and 2006 are available for viewing and download. Processing of North America data for several more years is underway. To enable users to process plumes in areas of special interest to them, the MINX program itself can be downloaded from the Open Channel Foundation website at https://www.openchannelsoftware.com/projects/MINX. Examples of MINX output for a particular scene are shown in Figs. 4 and 5. The area shown is located in central Alaska.

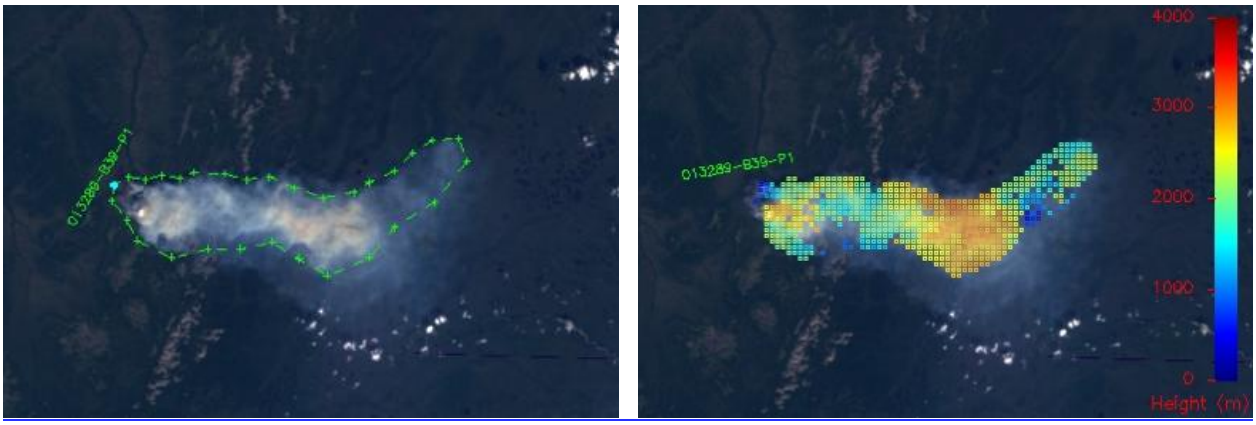

Figure 4. Left: MISR nadir camera image of a smoke plume in central Alaska, captured on 17 June 2002 during Terra orbit 13289. The green line surrounding the plume is a circumscribed boundary drawn by the operator using the MINX tool. Right: Map of retrieved heights generated by the MINX algorithm.

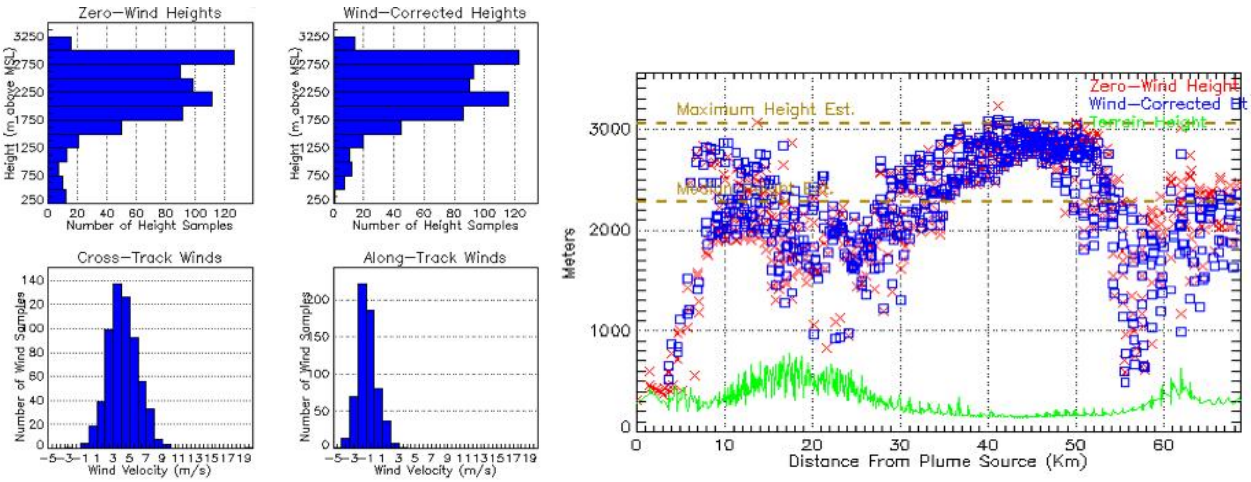

Figure 5. Left: Histograms of zero-wind heights, wind-corrected heights, cross-track and along-track wind speeds retrieved using MINX for the plume shown in Fig. 4. Right: Cross-sectional plot of heights as a function of distance from the source (red: zero-wind heights; blue: wind-corrected heights). The green line shows the terrain height.

4. PLUME HEIGHT CLIMATOLOGY DATA

4.1 Plume heights relative to the boundary layer for North America in 2002

A previous analysis using MINX has shown that over Alaska and the Yukon in summer of 2004, about 20% of the retrieved plume heights are above the atmospheric boundary layer (BL) [29]. An analysis of CALIOP data [30] suggested that smoke is only rarely transported above the BL. These apparently contradictory conclusions were addressed by Kahn et al. [29], who attributed the difference to the vastly greater horizontal coverage of MISR stereo imaging compared to the lidar. In this paper, we show initial results using MINX for North America (Alaska-Canada, the lower 48 states, and subtropical regions) for all of 2002. We explored the relationship between the plume height and the BL height calculated from Goddard EOS Data Assimilation System (GEOS-4) meteorological fields. We show three measures of plume heights: (1) the mode height for each plume, defined as the height with the largest number of pixels, (2) the best-estimated median height for each plume, defined as the median height after a plane is fitted to all successful height points within a plume, after removing all points more than 1.5 standard deviations from the plane, and (3) all individual heights within each plume.

The right hand plot in Fig. 6 shows the distribution of mode height-BL (black curve) and median height-BL (blue curve). The distribution of all individual heights-BL is overplotted in red. Plumes with a poor quality flag were excluded from the analysis. This resulted in removal of 16% of the cases for the 2002 dataset, leaving a total sample size of 404 plumes. For the three height metrics shown (mode, median, and all heights), 26%, 32%, and 35% of the heights are above the boundary layer, respectively. Using the same metrics, we also find that 9%, 10%, and 14% of the heights are more than 500 m above the boundary layer. Thus, the conclusions are to first order not sensitive to the height metric chosen.

4.2 Relationship of plume heights to atmospheric stability

Following up on the suggestion of Kahn et al. [1] (based on case studies) that plumes tend to concentrate near levels of enhanced stability, a statistical analysis was conducted on plumes in Alaska and the Yukon Territories during June-September 2004. A total of 692 plumes was included in the analysis. Atmospheres with strata of stable layers dominate at high latitudes, and in 87% of the cases analyzed the atmosphere had a well-defined stratified stable layer. Atmospheric stability S (e.g., in the right-hand panel of Fig. 1) was calculated from GEOS-4 data and is defined as the vertical lapse rate of potential temperature:

$$S = \frac{d\vartheta}{dz}, \quad \text{where } \vartheta = T\left(\frac{p_0}{p}\right)^{R/c_p} \tag{1}$$

T, p, and z are atmospheric temperature, pressure, and height respectively. R is the gas constant for dry air, c_p is the specific heat for dry air at constant pressure, and p_0 is the surface pressure. High values of S correspond to layers where the atmosphere is less likely to experience vertical mixing. Using the inflection point at the top of the stable layer as an operational definition of its height, Fig. 7 shows a histogram of the difference between the mode value of plume height and the height of the tops of the stable layers for this set of cases, along with a map of plume locations. A similar histogram is obtained when the median plume altitude is employed. We find that for stable atmospheres the representative (mode or median) plumes heights tend to be ~0.8 km below the top of the stable layer. To identify a stable layer, we specify that the difference in stability between GEOS-4 levels must be at least 1, and that the level of stability be between 0.75 and 7 km altitude. The latter condition is imposed because the proximity of layers in the lower troposphere, combined with the uncertainty in the highly averaged meteorological data, can lead to incorrect results. In the remaining cases, with neutral or convective atmospheres, the majority of plume altitudes were about 0.7 km below the height of the boundary layer, consistent with earlier findings [29]. Preliminary analysis of 2002 Alaska-Canada fires indicates that 20-30% of smoke plumes reached the free troposphere, consistent with results obtained for the 2004 fire season [29]. The fraction of smoke plumes injected above the BL was larger over the lower 48 states and subtropical regions (>30%).

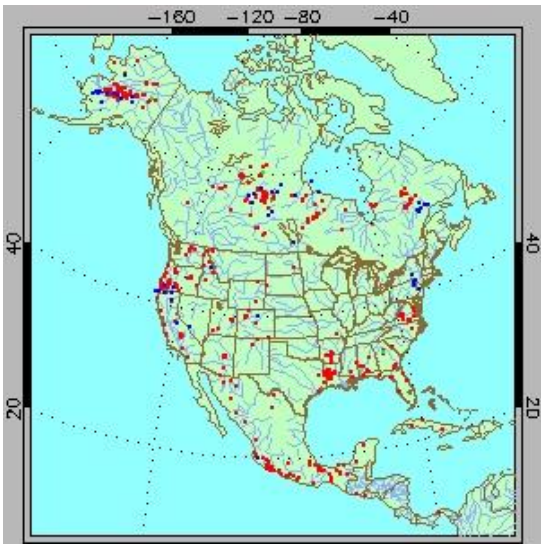

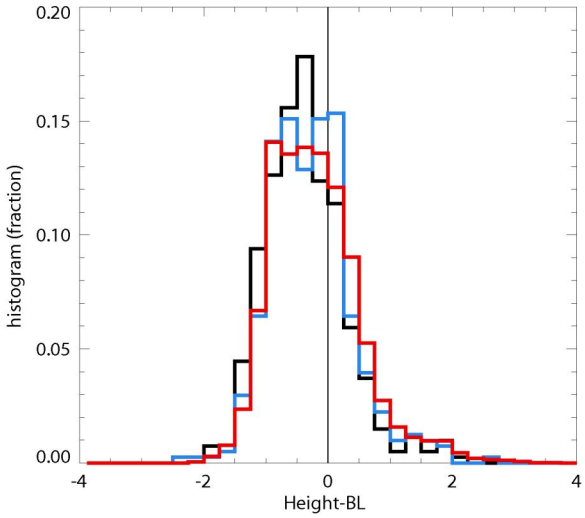

Figure 6. Left: Map of 2002 plumes for which height data were retrieved with MINX. Only the red dots (smoke plumes) are included in the reported statistics; the blue dots (detached smoke clouds) are not included. Right: Histogram of wind-corrected plume mode height-BL height (black) and median height-BL height (blue) for plumes detected by MISR and analyzed with MINX for North America in 2002. The distribution of all individual heights-BL is overplotted in red.

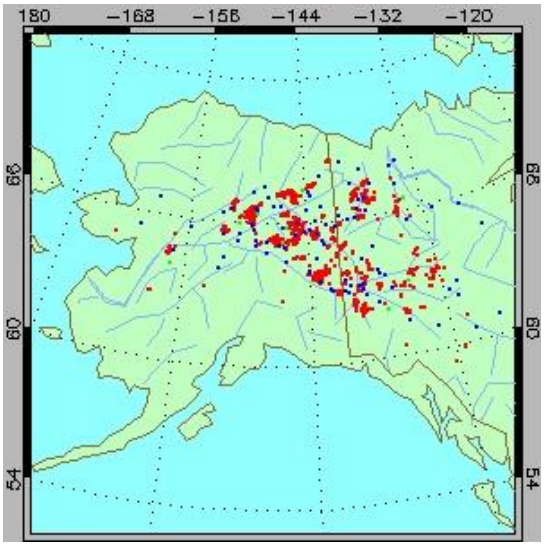

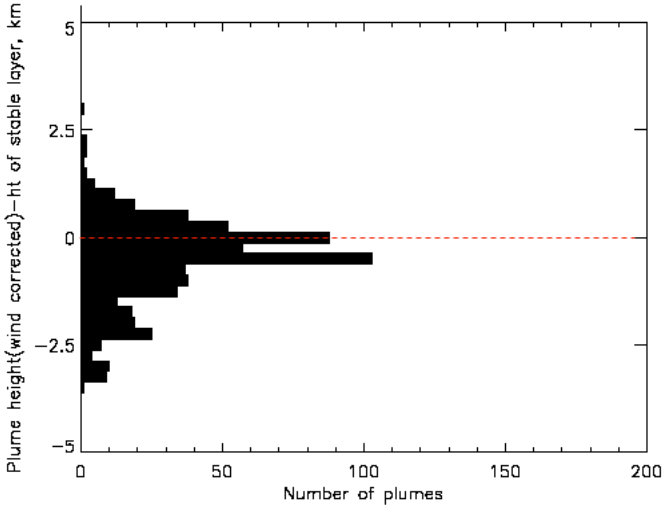

Figure 7. Left: Map of Alaska/Yukon plumes for summer 2004 (see Fig. 6 for legend). Right: Histogram of wind-corrected plume mode height-height of the top of the stable layer, generated from cases with well-defined layers of stability.

These findings have implications for the chemical transport simulations. Model studies conventionally distribute the trace gases and aerosols emitted by wildfires into the boundary layer, and rely on the model for the vertical and horizontal transport. Statistics from MISR-observed wildfire injection heights provide an observationally-constrained, more realistic representation of vertical distribution of biomass burning emissions in the model. Model simulations with this vertical distribution may improve our understanding of the long-range transport of wildfire emissions, and how this transport affects air quality and climate.

5. CONCLUSIONS

Global stereoscopic imaging is demonstrated to be a viable remote sensing complement to active atmospheric profiling for determining the heights of many smoke plumes and smoke clouds. Details of aerosol vertical profiles are best retrieved with lidar, but the wide horizontal coverage of stereo imagery enables the gathering of a large statistical

database of plume characteristics when sufficient spatial structure exists to enable multiangle pattern matching. The plume information archived in the standard MISR stereo product is now supplemented by the greater level of detail possible with the MINX quantitative analysis software tool. Analyses of data from 2002 and 2004 indicate that a significant fraction of plumes are lofted into the free troposphere. If a stable layer is present, the results presented here support earlier, case-study analysis [1] suggesting that its altitude can be used as a reasonable predictor of the level at which plumes level off. So far, regressions of plume altitudes with other environmental variables, e.g., fuel loading, plume area [29], and fire radiant energy [29], have not established meaningful correlations. Processing of a full 5 years of MISR data over North America using MINX is currently being completed under the auspices of the Plume Height Climatology Project, and the web site containing publicly available retrievals (see §3.2) will be updated as additional results are obtained.

ACKNOWLEDGMENTS

The research described in this paper was carried out at the Jet Propulsion Laboratory, California Institute of Technology, under contract with the National Aeronautics and Space Administration (NASA), and at the NASA Goddard Space Flight Center, Harvard University, and Washington State University. Funding from the US Environmental Protection Agency (EPA), the NASA Earth Observing System, and the NASA Applied Sciences, Atmospheric Composition, and Climate and Radiation Programs, is gratefully acknowledged. We thank Catherine Moroney for specialized runs of the MISR stereo processing code using oblique camera imagery, and Stacey Boland for coordination of the Plume Height Climatology Project. We appreciate the efforts of several individuals who used MINX for digitization of 2002 and 2004 MISR smoke plume data, including Rachel Morford, Harry Campbell, Kris Capraro, and Clare Averill.

REFERENCES

[1] Kahn, R.A., W.-H. Li, C. Moroney, D.J. Diner, J.V. Martonchik, and E. Fishbein, "Aerosol source plume physical characteristics from space-based multiangle imaging," *J. Geophys. Res.* **112**, D11205, doi:10.1029/2006JD007647 (2007).

[2] Colarco, P.R., M.R. Schoeberl, B.G. Doddridge, L.T. Marufu, O. Torres, and E.J. Welton, "Transport of smoke from Canadian forestfires to the surface near Washington, D.C.: Injection height, entrainment, and optical properties," *J. Geophys. Res.* **109**, D06203, doi:0.1029/2003JD004248 (2004).

[3] DeBell, L. J., R.W. Talbot, J.E. Dibb, J.W. Munger, E.V. Fischer, and S.E. Frolking, "A major regional pollution event in the northeastern U.S. caused by extensive forest fires in Quebec, Canada," *J. Geophys. Res.* **109**, D19305, doi:10.1029/2004JD004840 (2004).

[4] Peppler, R.A., C.P. Bahrmann, J.C. Barnard, J.R. Campbell, M.D. Cheng, R.A. Ferrare, R.N. Halthore, L.A. Heilman, D.L. Hlavka, N.S. Laulainen, C.J. Lin, J.A. Ogren, M.R. Poellot, L.A. Remer, K. Sassen, J.D. Spinhirne, M.E. Splitt, and D.D. Turner, "ARM Southern Great Plains Site observations of the smoke pall associated with the 1998 Central American fires," *Bull. Am. Met. Soc.* **81**, 2563-2591 (2000).

[5] Tanner, R.L., W.J. Parkhurst, M.L. Valente, K.L. Humes, K. Jones, and J. Gilbert, "Impact of the 1998 Central American fires on PM2.5 mass and composition in the southeastern United States," *Atmos. Environ.* **35**, 6539-6547 (2001).

[6] Gaffney, J.S., N.A. Marley, P. J. Drayton, P.V. Doskey, V.R. Kotamarthi, M.M. Cunningham, J.C. Baird, J. Dintaman, and H.L. Hart, "Field observations of regional and urban impacts on NO2, ozone, UVB, and nitrate radical production rates in the Phoenix air basin," *Atmos. Environ.* **36**, 825-833 (2002).

[7] Westerling, A.L., H. G. Hidalgo, D.R. Cayan, and T.W. Swetnam, "Warming and earlier spring increases western U.S. forest wildfire activity," *Science* **313**, 940-943 (2006).

[8] Brown, T.J., B.L. Hall, and A.L. Westerling, "The impact of twenty-first century climate change on wildland fire danger in the western United States: An applications perspective," *Clim. Change* **62**, 365-388 (2004).

[9] Chin, M., P. Ginoux, S. Kinne, O. Torres, B. Holben, B.N. Duncan, R.V. Martin, J.A. Logan, A. Higurashi, and T. Nakajima, "Tropospheric aerosol optical thickness from the GOCART model and comparisons with satellite and sunphotometer measurements," *J. Atmos. Sci.* **59**, 461-483 (2002).

[10] Bertschi, I.T., D.A. Jaffe, L. Jaeglé, H.U. Price, and J.B. Dennison, "PHOBEA/ITCT 2002 airborne observations of trans-Pacific transport of ozone, CO, VOCs, and aerosols to the Northeast Pacific: Impacts of Asian anthropogenic and Siberian boreal fire emissions," *J. Geophys. Res.* **109**, doi:10.1029/2003JD004200 (2004).

[11] Leung, F-Y., J.A. Logan, R. Park, E. Hyer, E. Kasischke, D. Streets, and L. Yurganov, "Impacts of enhanced biomass burning in the boreal forests in 1998 on tropospheric chemistry and the sensitivity of model results to the injection height of emissions," *J. Geophys. Res.* **112**, D10313, doi:10.1029/2006JD008132 (2007).

[12] Cofer, W.R., E.L. Winstead, B.J. Stocks, L.W. Overbay, J.G. Goldammer, D.R. Cahoon, and J.S. Levine, "Emissions from boreal forest fires: are the atmospheric impacts underestimated?" *Biomass Burning and Global Change* (ed. J.S. Levine, MIT Press, Cambridge, MA), 834-839 (1996).

[13] Lavoue, D., C. Liousse, H. Cachier, B. J. Stocks, and J. G. Goldammer, "Modeling of carbonaceous particles emitted by boreal and temperate wildfires at northern latitudes," *J. Geophys. Res.* **105**, 26871-26890 (2000).

[14] Fromm, M.D., and R Servranckx, "Transport of fire smoke above the tropopause by supercell convection," *Geophys. Res. Lett*. **30**, 1542 (2003).

[15] Fromm, M., O. Torres, D. Diner, D. Lindsey, B. Vant Hull, R. Servranckx, E. P. Shettle, and Z. Li, "Stratospheric impact of the Chisholm pyrocumulonimbus eruption: 1. Earth-viewing satellite perspective," *J. Geophys. Res*. **113**, D08202, doi:10.1029/2007JD009153 (2008).

[16] Winker, D.M., W.H. Hunt, and M.J. McGill, "Initial performance assessment of CALIOP," *Geophys. Res. Lett.* **34**, L19803, doi:10.1029/2007GL030135 (2007).

[17] Diner, D.J., J.C. Beckert, T.H. Reilly, C.J. Bruegge, J.E. Conel, R.A. Kahn, J.V. Martonchik, T.P. Ackerman, R. Davies, S.A.W. Gerstl, H.R. Gordon, J-P. Muller, R.B. Myneni, P.J. Sellers, B. Pinty, and M. Verstraete, "Multi-angle Imaging SpectroRadiometer (MISR) instrument description and experiment overview," *IEEE Trans. Geosci. Remote Sens.* **36**, 1072-1087 (1998).

[18] Jovanovic, V.M., M.A. Bull, M.M. Smyth, and J. Zong, "MISR in-flight camera geometric model calibration and georectification performance," *IEEE Trans. Geosci. Remote Sens*. **40**, 1512-1519 (2002).

[19] Moroney, C., R. Davies, and J.-P. Muller, "Operational retrieval of cloud-top heights using MISR data," *IEEE Trans. Geosci. Remote Sens*. **40**, 1541-1546 (2002).

[20] Muller, J.-P., A. Mandanayake, C. Moroney, R. Davies, D. J. Diner, and S. Paradise, "MISR stereoscopic image matchers: Techniques and results," *IEEE Trans. Geosci. Remote Sens*. **40**, 1547-1559 (2002).

[21] Naud, C., J.-P. Muller, M. Haeffelin, Y. Morille, and A. Delaval, "Assessment of MISR and MODIS cloud top heights through inter-comparison with a back-scattering lidar at SIRTA," *Geophys. Res. Lett.* **31**, L04114 (2004).

[22] Naud, C.M., J.-P. Muller, E. E. Clothiaux, B. A. Baum, and W. P. Menzel, "Intercomparison of multiple years of MODIS, MISR and radar cloud-top heights," *Annales Geophysicae* **23**, 1–10 (2005).

[23] Marchand, R.T., T.P. Ackerman, and C. Moroney, "An assessment of Multi-angle Imaging SpectroRadiometer (MISR) stereo-derived cloud top heights and cloud top winds using ground-based radar, lidar and microwave radiometers," *J. Geophys. Res*. **112**, D06204, doi: 0.1029/2006JD007091 (2007).

[24] Horváth, Á ., and R. Davies, "Simultaneous retrieval of cloud motion and height from polar-orbiter multiangle measurements," *Geophys. Res. Lett.* **28**, 2915–2918 (2001).

[25] Zong, J., R. Davies, J.-P. Muller, and D. J. Diner, "Photogrammetric retrieval of cloud advection and top height from the Multi-angle Imaging SpectroRadiometer (MISR)," *Photogramm. Eng. Remote Sens.* **68**, 821– 829 (2002).

[26] Stenchikov, G., N. Lahoti, D.J. Diner, R. Kahn, P.J. Lioy, and P.G. Georgopoulos, "Multiscale plume transport from the collapse of the World Trade Center on September 11, 2001," *Environ. Fluid. Mech.* **6**, 425-450 (2006).

[27] Nelson, D.L., Y. Chen, D.J. Diner, R.A. Kahn, and D. Mazzoni, "Example applications of the MISR INteractive eXplorer (MINX) software tool to wildfire smoke plume analyses," *Proc. SPIE*, this conference (2008).

[28] Mazzoni, D., J.A. Logan, D. Diner, R. Kahn, L.L. Tong, and Q.B. Li, "A data-mining approach to associating MISR smoke plume heights with MODIS fire measurements," *Rem. Sens. Environ*. **107**, 138-148 (2007).

[29] Kahn, R., Y. Chen, D.L. Nelson, F.Y. Leung, Q.B. Li, D.J. Diner, and J.A. Logan, "Wildfire smoke injection heights: Two perspectives from space," *Geophys. Res. Lett.* **35**, L04809, doi:10.1029/2007GL032165 (2008).

[30] Labonne, M., F.-M. Bréon, and F. Chevallier, "Injection height of biomass burning aerosols as seen from a spaceborne lidar," *Geophys. Res. Lett.* **34**, L11806, doi:10.1029/2007GL029311 (2007).